LA-UR- 98- 4231

Title: MEASUREMENT OF NEUTRON TOTAL CROSS SECTIONS IN SUPPORT OF THE APT PROGRAM

Author(s): W. P. Abfalterer
R. C. Haight
G. L. Morgan
F. B. Bateman
F. S. Dietrich
R. W. Finlay

Submitted to: 15th International Conference on the Application of Accelerators in Research and Industry, November 4-7, 1998, Denton, TX

Los Alamos
NATIONAL LABORATORY

DISCLAIMER

Measurement of Neutron Total Cross Sections in Support of the APT Program

W. P. Abfalterer, R. C. Haight, G. L. Morgan, and F. B. Bateman
Los Alamos National Laboratory, Los Alamos, NM 87545 USA

F. S. Dietrich
Lawrence Livermore National Laboratory, Livermore, CA 94551 USA

R. W. Finlay
Ohio University, Athens, OH 45701 USA

We have completed a new set of total cross section measurements of 37 samples spanning the periodic table. We employed the same technique as in a previous measurement (1), with refinements intended to allow measurements on separated isotopes, and with improved systematic error control. The goal of the new measurement was 1 % statistical accuracy in 1 % energy bins with systematic errors less than 1 %. This was achieved for all but the smallest samples, for which the statistical accuracy was as large as 2 % in 1% bins.

INTRODUCTION

Neutron total cross sections are the most fundamental quantity describing the interactions of neutrons with nuclei. If there is any interaction at all, including elastic and all nonelastic interactions, then it is reflected in the total cross section. Yet the data base of total cross sections has significant uncertainties and, in regions, significant gaps. Therefore we undertook this extensive program to measure these cross sections.

These measurements were supported by the Accelerator Production of Tritium (APT) project as part of a program to improve the physics in the modeling code (LAHET) used in the design of the APT target and other parts of the facility. The new data, along with those of (1), are being used in the development of a global optical potential from 20 to 2000 MeV.

The goal of the new measurements was 1 % statistical accuracy in 1 % energy bins with systematic errors less than 1 %. This was achieved for all but the smallest samples, for which the statistical and systematic accuracy was as large as 2 % in 1 % energy bins. The data will be given to the National Nuclear Data Center at the Brookhaven National Laboratory in 1% energy bins. However, the energy resolution is significantly better than this at low energies.

We measured the total neutron cross section of 37 materials at the Los Alamos WNR spallation source. We employed the same techniques as in (1), with refinements intended to allow measurements on separated isotopes and other materials only available in small quantities.

Samples were the APT spallation target material W; medium-mass structural materials Ti, V, Cr, Mn, Fe, Co, and Ni; the actinides Th and depleted U; the materials for global optical model development F, Mg, P, S, K, Y, Mo, In, Au, Hg, and natural Pt; the light nuclei Li, B, and C; the separated isotopes of light nuclei ^{6}Li, ^{7}Li, ^{10}B, ^{11}B, and ^{13}C; the medium- and heavy-mass separated isotopes ^{54,56}Fe, and ^{182,183,184,186}W; the few-nucleon nuclei H and D.

Total neutron cross sections were determined by measuring the transmitted neutron beam through a known amount of sample material in comparison to the transmitted beam without sample. If N_o is the number of counts without a sample, and N_i is the number of counts with a sample interposed between neutron source and detector, then the transmission is given by:

$$T = \frac{N_i}{N_o} = e^{-nl\sigma_T}, \qquad (1)$$

where n denotes the number of atoms per unit volume and l the sample length. The total neutron cross section σ_T can then be determined as

$$\sigma_T = -\frac{1}{nl} \ln \frac{R_i - B_i}{R_o - B_o}. \qquad (2)$$

R_i and R_o denote the normalized sample-in and sample-out rates respectively, and B_i, B_{out} the normalized background rates.

Therefore, for a successful total neutron cross section measurement the following ingredients were needed: An accurate measurement of the areal density (nl), knowledge of the background rates and an accurate normalization of sample-in and sample-out fluences. Thus we required a well defined experimental geometry, stable detectors and electronics, and a solid understanding of systematic effects such as electronic dead time.

TECHNIQUE

Total cross sections were measured in a good-geometry (i.e., a geometry that minimizes in-scattering) transmission experiment with neutrons up to 600 MeV emanating at 30 degrees from the LANSCE WNR TARGET 4 white neutron source. The white neutron source was realized by bombarding a water-cooled tungsten target with 800 MeV protons.

The neutron energy was determined by standard time-of-flight techniques. For details on the proton beam structure and time-of-flight technique see (2).

This experiment is distinguished from (1) in a number of ways. Instead of one detector, two detectors were employed with different thicknesses in order to increase the count rate at the high end of the neutron spectrum, and also to have a check on systematic errors. Our count rate was further increased by a factor 2.5 because of an increased beam repetition rate (macropulse).

The sample wheel and detector set-up are shown in Fig. 1. For a more detailed description see (2). Neutrons traveled from the tungsten production target through vacuum to the shutter exit window and then through air for the remainder of the flight path. A 10.16-cm-thick piece of polyethylene

Views of the apparatus for measuring neutron total cross sections

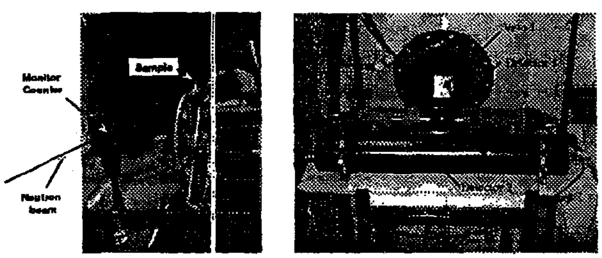

Looking downstream near sample changer — *View of detectors at 40-m flight station*

FIGURE 1. The left-hand picture shows the monitor and sample wheel set-up, and the right-hand picture shows the veto and detector set-up. The second veto counter is hidden behind detector 2.

(CH_2) was used to harden the beam for all but the hydrogen and deuterium cross section measurements. This greatly reduced the over-all count rate in the detectors but had little effect on the rates above 100 MeV where high statistical accuracy is most difficult to achieve. A 1.27-cm-thick piece of lead was used to attenuate the gamma burst. Two sets of sweeping magnets removed charged particles upstream of the sample. A horseshoe magnet swept charged particles out of the flight path immediately after the sample. The sample was situated in such a way as to completely shadow the detectors. Sample diameters were typically 2.54 cm but spanned a range from 2.117 to 3.810 cm.

Data were taken in 25 sets referred to as "wheels"; these were distinguished by the samples mounted on the rotating sample changer which was a wheel 63.5 cm in diameter with eight positions for samples including the "open" sample.

In order to assess the beam stability we continuously checked the ratio of sample-out detector to monitor, and discarded data taken during erratic beam conditions.

Figure 2 shows the transmission through the shadow bar for detectors 1 and 2 in comparison to the dead-time corrected and normalized open beam (sample-out) spectrum.

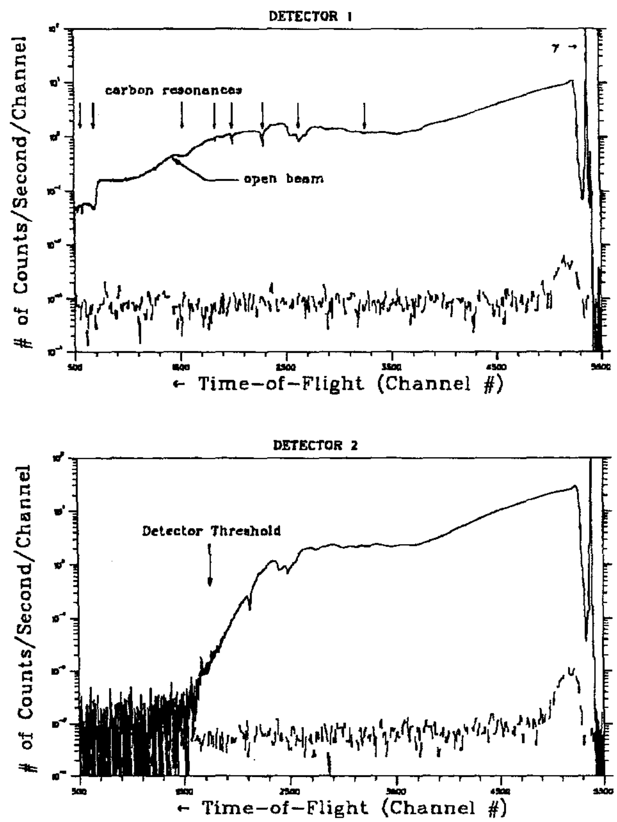

FIGURE 2. Open beam (i.e. sample-out) and shadow bar time-of-flight spectra after dead time corrections for detectors 1 and 2. These show from right to left, the gamma flash, the fast neutron spectrum modified at the lower energies by transmission resonances in carbon (CH_2 filter), the detector threshold, and the time independent background.

The basic philosophy and consequent approach to this experiment were to gain a clear understanding of the systematic uncertainties involved, given the neutron beam and flight path geometry parameters. This is one of the reasons that two independent detector systems were employed. The detectors were distinguished by different bias settings, different types of discriminators, and considerably different count rates for a given sample.

Detector 1 was a 8.9 × 8.9 cm, 1.27-cm-thick piece of BC404. Detector 1 was located at 37.70 ± 0.01 m from the neutron source. Detector 2 was of the same construction, the thickness of the scintillator being 5.08 cm instead. Detector 2 was located at 39.61 ± 0.02 m.

Veto counters just in front of the neutron detectors were used to reject charged particles produced by neutron reactions on air in the flight path or other materials upstream of each detector. The monitor counter consisted of a circular plastic scintillator, 5.08 cm diameter and 0.159 cm thick.

Good agreement between results from detectors 1 and 2 gave confidence in the approach. In addition to the differences in the detectors and the electronics, the individual de-

detector count rate characteristics were investigated by varying the thickness of a particular type of sample. Finally, as a check on the long-time stability of the system several samples were remeasured as far apart as half a year, and again excellent agreement was obtained.

ELECTRONICS AND DATA ACQUISITION

The essential principles of the electronics are as follows: Figure 3 shows a simplified time line. Logic T_0's associated

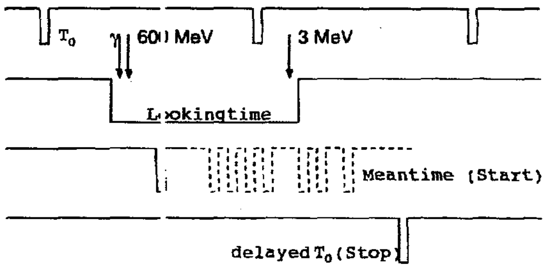

FIGURE 3. Simplified Time Line.

with the proton beam burst arrived at evenly spaced 1.8 μs time intervals, defining a time frame. These are used as stops on the TDC clocks. We checked for a busy condition at the beginning of a time frame. If the system was not busy, then it was free to start the clock with a neutron event. This arrangement allowed a clean separation of dead time corrections:

- "analytic" dead time - a neutron event within a frame prevents subsequent events within that frame from being analyzed.
- a correction $\frac{T_0}{T_{0\,Live}}$ for busy frames.

The complete electronics setup is discussed in (2). Neutron-energy high and low thresholds for detector 1 were set to give useful data above 2.7 and 8 MeV, respectively. The detector 2 threshold gave data above E_n = 10 MeV. No high bias was set for detector 2. In the final data analysis, detector 1 was used above a neutron energy where the statistical uncertainty was better than 1 %, typically 3 - 6 MeV depending on the sample. Detector 2 was used above 10 MeV.

Data were acquired on a given sample for 20 seconds after which the target wheel was rotated to another position. This rapid sample cycling minimizes effects of drifts in the beam spatial and energy profiles.

SAMPLE CHARACTERISTICS

We dealt with several categories of samples: metallic samples, encapsulated natural powder samples, encapsulated isotopic powders, encapsulated isotopic solids, encapsulated liquids, pressed powders, solid hydrogen and fluorine compounds, and sintered samples. All samples were cylindrical. A detailed description of the sample characteristics is presented in in (2).

As we discovered, uncertainties in the areal density of the samples are in many instances the main contributing factor to the systematic uncertainty in the determination of the final total neutron cross sections. Areal density was therefore determined in as many as three ways: by physical measurements of mass and dimensions, by a bulk density measurement by water immersion coupled with a length measurement, and by gamma-ray attenuation.

DATA ANALYSIS

Raw spectra were first processed by employing the so-called analytic dead-time correction. This correction is due to the fact that low-energy neutrons have a smaller probability of being counted than high-energy neutrons because the first-arriving TDC start pulse within a given frame blocks the system from processing later events within that time frame. Reference (3) gives a detailed description of this effect and the necessary corrections for it.

The remaining dead-time of the TDC system is taken care of by scaling the total number of logic T_0's, the number of T_0's while the system was alive (called $T_{0\,Live}$), and the number of times a conversion in progress was aborted by a veto-counter event (denoted v). The correction was accomplished by multiplying the analytic-dead-time correction by the factor $T_0/(T_{0\,Live}-v)$.

Using charged-particle veto counters results in systematic changes in cross sections that are typically in the 0.5 % range. However, it is necessary to account for accidental coincidences between the veto and main detectors in order to avoid a count-rate-dependent systematic error.

The time-independent background was then subtracted from the corrected spectra, and time-of-flight converted to energy in 1 % bins. For the time-to-energy transformation well-known carbon resonances were used to determine the flight path for detector 1 and detector 2.

Finally, spectra were normalized to the monitor counts, and the total neutron cross section was calculated with all statistical uncertainties properly propagated.

SUMMARY OF SYSTEMATIC EFFECTS

For a detailed discussion of systematic effects see (2). We will only discuss here detector count rate stability , and detector 1 vs. detector 2 consistency.

Detector count rate stability: We tested the count rate stability of a given detector and the electronics associated with it by measuring the total neutron cross section of elements with different sample length as in the case of oil-hardened tool steel, Teflon, and also varying length carbon samples. Systematic differences for the Teflon samples and steel samples were of the order of 0.5 %. In the case of the carbon samples, detector 2 showed better consistency above 100 MeV for the thinnest carbon sample (C-short), where the detector-1 systematic differences were as high as 1.5 % when compared to the longer carbon samples. We attribute these differences to a slightly better detector 2 count-rate stability, and therefore only used detector 2 data above 100 MeV for $^{6,7}Li$, $^{10,11}B$, and ^{13}C.

Figure 4 shows the ratio of cross sections using detector 2 for the 2 cm and 9 cm carbon samples. The attenuations of the two samples at 300 MeV (near the cross section minimum) are approximately 20 % for the long carbon sample and 4.7 % for the short sample. The latter is comparable to the attenuation of the thinnest sample of interest, ^{11}B, which has an attenuation of about 4.5 % at 300 MeV. The slight overall deviation of the ratio from unity (approximately 0.5 %) is within the uncertainty of the sample density determinations. There is no evidence for an energy dependence of the ratio beyond the level of about 0.5 %.

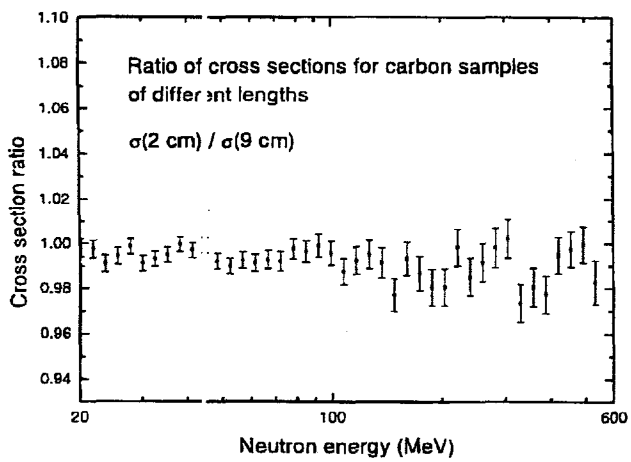

FIGURE 4. The detector 2 cross section ratio for the 2 cm and 9 cm carbon samples: The results were binned in 8 % bins in order to get adequate statistics.

Detector 1 vs. detector 2 consistency: The consistency of the total neutron cross sections as a function of count rate as determined for detector 1 and detector 2 was checked by comparing the cross section differences between detector 1 and detector 2 by varying the length of carbon samples from 2 to 15 cm. Only for the thinnest carbon sample did we notice a discrepancy above 100 MeV of the order of 1.5 - 2 %. This was another reason for only using detector-2 data above 100 MeV for the samples mentioned in the previous paragraph.

RESULTS

Figure 5 depicts a sampling across the periodic table of the total neutron cross sections measured in this experiment. Compound resonances arising from the interference of many nearby states can be seen in the cross sections of the lighter elements such as Mg, S, and P, whose analysis allows the extraction of level density information. The giant resonances seen in the cross sections of the medium and heavier elements are the result of potential scattering, which arises from the interferences between the incident wave function and the wave transmitted through the nuclear potential.

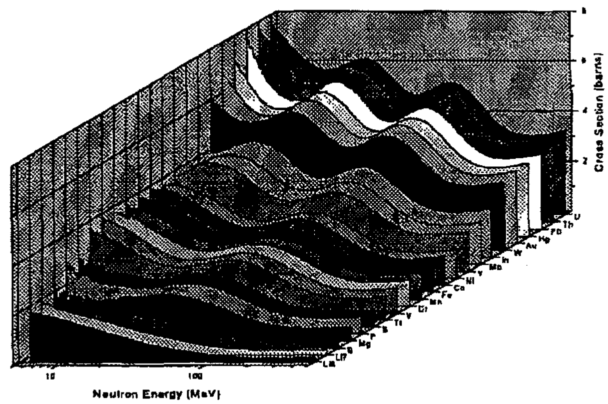

FIGURE 5. Results for 22 of the 37 samples measured.

The results for the total cross section difference deuterium-hydrogen (d-h) have been used to test the Faddeev description of the n+d total cross section between 10 and 300 MeV (4).

ACKNOWLEDGMENTS

Thanks to Sina and Thomas Manista from Dupont for graciously providing us with high purity Teflon samples and trying to explain its physical and chemical properties, to Poly Hi Solidur for the high purity polyethylene samples, to 3M for the C_8F_{18}, and the Y-12 Development Division for the LiH samples. Special thanks to Dale Sivils from CST-12 for performing the chemical analysis of the octane and C_8F_{18}, and to Rose Gray and Alex Herrera for x-raying a number of samples. Another special thanks to Art Bridge and Lloyd Hunt for all their tireless technical support in keeping the sample wheel turning and the experiment going, and to Steve Wender for operations support.

Work performed in part under USDOE contracts W-7405-ENG-48 (LLNL), W-7405-ENG-36 (LANL), and DE-FG02-93ER40756 (Ohio University).

REFERENCES

1. R. W. Finlay, W. P. Abfalterer, G. Fink, E. Montei, T. Adami, P. W. Lisowski, G. L. Morgan, and R. C. Haight, Phys. Rev. **C47**, 237 (1993).
2. W. P. Abfalterer, F. S. Dietrich, R. C. Haight, G. L. Morgan, F. B. Bateman, and R. W. Finlay, LA-UR-98-4058 (1998).
3. M. S. Moore, Nucl. Instrum. Methods **169**, 245 (1980).
4. W. P. Abfalterer, F. B. Bateman, F. S. Dietrich, Ch. Elster, R. W. Finlay, W. Glöckle, J. Golak, R.C. Haight, D. Hüber, G. L. Morgan, and H. Witala, Phys. Rev. Lett., **81**, 57 (1998).